

MATHEMATICAL MODELING APPROACH FOR DELINEATING
LANDSLIDE HAZARDS IN WATERSHEDS

By

Timothy J. Ward
Assistant Professor of Civil Engineering
Colorado State University

Ruh-Ming Li
Associate Professor of Civil Engineering
Colorado State University

and

Daryl B. Simons
Associate Dean for Engineering Research and
Professor of Civil Engineering
Colorado State University

INTRODUCTION

Landslides pose an ever present threat to man's activities in hilly or mountainous watersheds. In addition to interfering with timbering, road building, mining, recreation, or second home development, landslides can provide large amounts of sediment to stream channels. This sediment can then lower water quality, increase flood hazards, and affect fisheries. Landslides are often initiated by man's activities or by natural events such as rainfall or earthquakes. In order to avoid triggering landslides and provide better scheduling of watershed activities to bypass potential landslide sites, methodologies are needed for delineating landslide hazards.

Landslides in watershed soils are a result of a combination of several interacting factors including soil strength, soil depth, groundwater, slope inclination, and vegetative influences. This paper presents an approach for delineating potential landslide areas based on such factors using a common geotechnical model. Using a watershed modeling approach the model, based on physical characteristics is developed and applied to a selected watershed. The results are encouraging suggesting that this approach may prove useful to the land use manager.

CURRENT APPROACHES

There are many approaches to landslide potential delineation. These approaches include on-ground monitoring, remote sensing techniques, factor overlay methods, statistical models, and geotechnical process models.

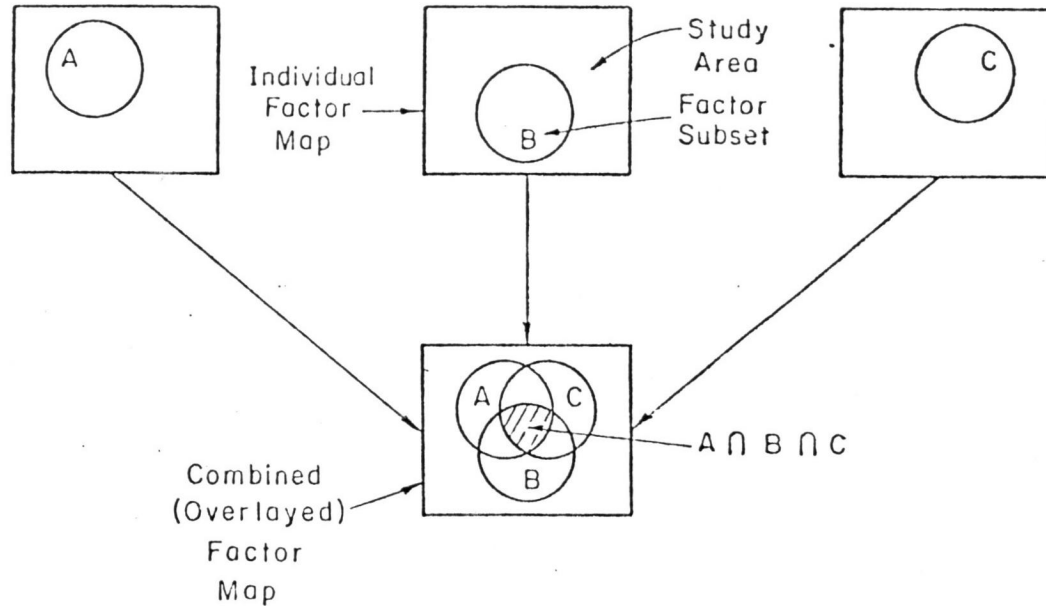
On-ground monitoring consists of utilizing installed measuring devices such as strain gages and down hole tilt meters. This type of approach is extremely useful for checking suspected landslide zones but is limited in aerial coverage because of cost of installation and maintenance. Chang (1971) summarized many of these techniques. Takada (1968) and Takeuchi (1971) provided two examples of applications of different methods.

Remote sensing coupled with pattern recognition techniques provide a means for surveying large areas. In this approach, remotely sensed data, particularly aerial photography such as black and white, color infrared, and multiband spectral, can be analyzed for features distinctive of landslide hazards (Liang and Belcher, 1958; Poole, 1969, 1972; McKean, 1977). This analysis, a type of the more general pattern recognition, can be quite effective if landslide hazards are manifested in surface characteristics that can be photographed. However, it is not always the situation since landslides often result from deep seated factors not visible on the ground surface.

The most common delineation method concurrently in use is factor overlay or a combination of landslide producing elements. Krynine and Judd (1957) noted that landslides occur in a regional framework, or that certain factors common to a region contribute to landsliding. Baker and Chieruzzi (1959) expanded this concept to develop a physiographic classification of landslide hazards based on topography, erosional development, and associated rock types. Blanc and Cleveland (1968) were two of the first to attempt delineating landslides by use of selected factors. Evans and Gray (1971) presented a methodology for mud slide risk delineation in Southern Ventura County, California. Cleveland (1971) summarized and presented those factors important in regional landslide prediction. His factors include precipitation, rock strength, vegetation effects, slope, and stream pattern. The approaches described by Nilsen and Brabb (1973) and the Building Research Advisory Board (1974) follow this systematic methodology using landslide factors. In this approach, certain factors related to landslide occurrence are individually delineated. For example, if landslides occur where steep slopes, weak earth materials, and water are all coincident, then these factors should be used as slope stability indicators. Areas where factors coincide can then be classified as a hazard potential. Simons and Ward (1976) summarized this approach as the factor overlay method or set theory approach to hazard delineation as presented in Figure 1. Although not explicitly stated in delineation schemes, this idea is the basis for most techniques.

The factor overlay approach is conceptually correct since it recognizes that landslides are a combination of different factors. However, this approach is subjective and nonsensitive to dynamic inputs. Subjectivity results from a lack of defined guidelines for developing and weighting various factors. Nonsensitivity occurs because static factors are usually considered while dynamic factors, such as groundwater fluctuations, are excluded. Factor overlay can be improved if standardized guidelines are developed, dynamic factors are incorporated, and realistic weighting functions are used. Simons and Ward (1976) presented a numerical approach to the factor overlay technique that may help quantify the relative importance of each factor.

Another method of potential delineation is use of empirically developed models. These models, developed through statistical analyses of measurable data, attempt to provide a numerical value related to slope stability. Multiple regression and discriminant function analyses are common techniques for developing such relationships (Jones, Embury and Peterson, 1961; Waltz, 1971). Empirically derived relationships have a major drawback since they require large amounts of data to develop the equations. Such data is usually temporally and spatially static. Temporally static implies the developed relationship is applicable to a limited time span during which data was collected and, therefore, does not represent changing conditions. Spatially static



Potential	Set
High	$A \cap B \cap C$
Medium	$A \cap B$; $B \cap C$; $A \cap C$; A ; B ; C
Low	$A \cup B \cup C$ (i.e. not in A, B, or C)

\cap - Intersection of Subsets

\cup - Union of Subsets

Figure 1. Set theory approach to landslide potential classification (from Simons and Ward, 1976).

implies the method is applicable to a limited area and transfer to other areas may not be warranted.

A final type of landslide hazard delineation methodology is based on geotechnical models. Geotechnical models are derived from observed natural phenomena and basic laws of physics, and are representative of the physical process being studied. Geotechnical models of slope stability relate the forces acting on the hill slope. One set of forces, predominated by gravity, acts to move earth materials downslope. The other set of forces, predominated by the shear strength of the earth materials, resists the driving gravity forces. When driving forces exceed resisting forces, a landslide occurs. Geotechnical models have been developed and modified to account for primary factors in landslide occurrence such as soil strength, groundwater influences, vegetative effects, and slope inclination. Because geotechnical models represent actual field conditions they can be used to analyze the response of a hill slope to temporally and spatially varying factors. Simplifying assumptions can yield a method for determining the probability of a landslide. Because of the ability to account for several temporally and spatially varying contributing factors in a nonsubjective, physically meaningful manner, geotechnical models are promising methods for landslide potential delineation.

FACTOR OF SAFETY DELINEATION MODEL

Model Selection

The analysis presented in this paper is applicable to translational or planar types of landslides in soil masses. Rock masses require a more complex analysis because of their response to the geometry of failure planes, and are not considered here.

Various types of slope stability models exist. Two basic types are the infinite slope and finite slope models, each derived by a different set of assumptions (Lambe and Whitman, 1969). Common to both types is the formation of a factor of safety equation that consists of a ratio of resisting to driving forces of

$$FS = \frac{R}{D} \quad (1)$$

where FS = factor of safety; R = resistive forces; and D = driving forces.

Resistive forces are related to soil strength and vegetative parameters while the primary driving force is the downslope weight of the soil mass. If resistance is less than the driving force, then the factor of safety is less than one indicating failure.

The infinite slope model of slope stability is primarily applicable to failure occurring along planar type surfaces such as translational slides. The model presented in this paper consolidates and refines ideas presented by several researchers (Brown and Sheu, 1975; O'Loughlin, 1974; Simons, Ward, and Li, 1976; Swanson, et al., 1973). These developments were further studied by Ward (1976) to yield the model's present form. Because finite slope formulations also relate the same resisting and driving force elements, the model can estimate the failure potential for other landslide types such as rotational slumps.

Derivation of Model Equations

Derivation of the equations of static equilibrium for an infinite slope is relatively easy (Brown and Shen, 1975; Lambe and Whitman, 1969; O'Loughlin, 1974). The derivation presented here is similar to those given by previous authors but with changes in the formulation and simplification of the basic model. An idealized infinite slope consisting of a single soil type with isotropic properties resting on a bedrock interface is shown in Figure 2. This situation is similar to residual soil slopes found in forested watersheds and most hilly or mountainous terrain.

The shear strength of a soil can be represented by the Coulomb equation of

$$\tau = \bar{c} + \bar{\sigma} \tan \bar{\phi} \quad (2)$$

where τ = shear strength; \bar{c} = effective cohesion intercept; $\bar{\sigma}$ = effective normal stress; and $\bar{\phi}$ = effective angle of internal friction.

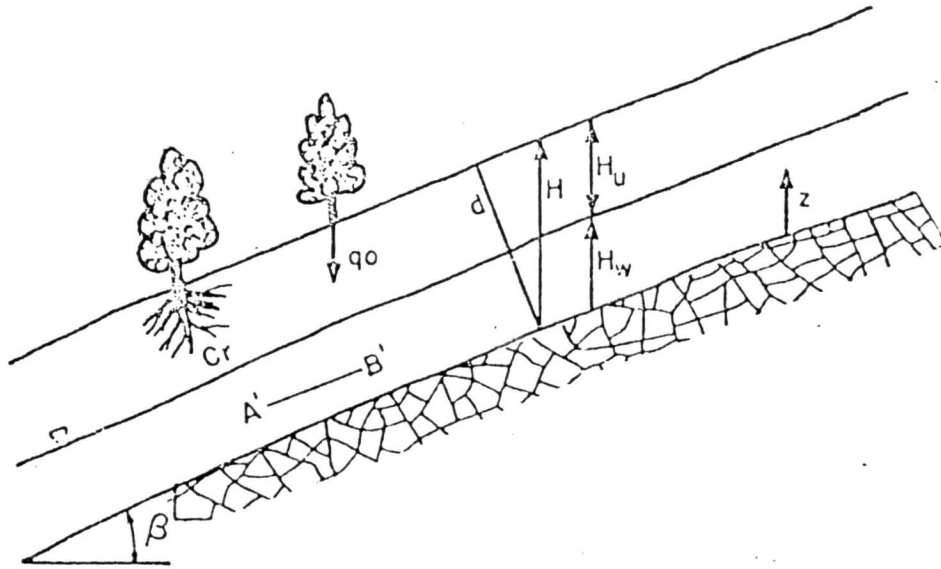


Figure 2. Idealized infinite slope.

Equation 2 is applicable to drained soil strength conditions and represents resisting forces contributed by the soil mass. Components of \bar{c} and $\bar{\phi}$ (hereafter, the overbar will be dropped) are intrinsic strength characteristics of soil and represent interaction of soil factors.

Analysis of Figure 2 aids evaluation of $\bar{\sigma}$. Normal stress on plane A' - B' located at a distance, Z, above the bedrock surface in the soil mass can be easily solved if the plane is assumed parallel to soil and bedrock surfaces and is located between $Z = 0$ and $Z = H_w$. The total normal stress, σ , on this plane can be written as

$$\sigma = \sum_{i=1}^n \gamma_i \Delta z_i \quad (3)$$

where γ_i = unit weight of layer i ; and Δz_i = thickness of layer i .

In this case $n = 2$ for the saturated and unsaturated soils but can be expanded to a multilayer case. However, in many residual soils, assumption of a single soil type is often valid (Lumb, 1970). The geometry and other important factors can be used to evaluate σ . The normal stress on plane A' - B' is composed of stresses from soil weight and tree surcharge. Soil weight per area component is $(H_u \cos \beta \gamma)$ for the soil above water table level and $[(H_w - Z) \cos \beta \gamma_{sat}]$ for soil below water table level. Normal force per area supplied by tree surcharge is $(q_0 \cos \beta)$. Assuming the contact surface as a unit squared the area enables the normal stress to be written as

$$\sigma = [q_0 \cos \beta + (H_w - Z) \cos \beta \gamma_{sat} + H_u \cos \beta \gamma] \cos \beta \quad (4)$$

In Equation 4 the area upon which the normal force acts is defined as $\cos \beta$ times a unit area. Since $H_u = H - H_w$, Equation 4 can be converted to

$$\sigma = H \cos^2 \beta [q_0/H + \gamma_{\text{sat}} (M-Z^*) + \gamma (1-M)] \quad (5)$$

where $M = \frac{H_w}{H}$ = relative groundwater height and $Z^* = \frac{Z}{H}$ = relative position from bedrock surface.

Because groundwater is present, the buoyancy effect of pore water pressures must be considered in Equation 4. From the effective stress concept the relationship between total and effective normal stress in soil mass components is

$$\bar{\sigma} = \sigma - u \quad (6)$$

where u = the pore water pressure. Hydrostatic pressure can be formulated as

$$u = H(M-Z^*) (\cos^2 \beta) \gamma_w \quad (7)$$

Combining and simplifying Equations 5, 6, and 7 yields

$$\bar{\sigma} = H \cos^2 \beta [q_0/H + (\gamma_{\text{sat}} - \gamma_w) (M-Z^*) + \gamma(1-M)] \quad (8)$$

Consequently, the shear resistance equation becomes

$$\tau = c + H \cos^2 \beta [q_0/H + (\gamma_{\text{sat}} - \gamma_w) (M-Z^*) + \gamma(1-M)] \tan \phi \quad (9)$$

The cohesion term, c , in Equation 9 has two components in forested watersheds--soil cohesion and tree root cohesion. Gray (1970, 1978) described several ways that vegetation enhances slope stability. One of these is anchoring soil to underlying strata. Endo and Tsuruta (1968) and O'Loughlin (1974) showed that anchoring can be represented in the FS equation as a cohesion term, C_r . The cohesion term, c , can then be replaced by terms for soil cohesion, C_s , and root cohesion, C_r .

A similar analysis can be made for shear stress induced on the plane. Shear stress is composed of loads resulting from the weight of the soil mass, tree surcharge, and wind shear in trees imparted to the soil mass. Seismic loading is not considered. Because air flow usually conforms to ground surfaces or treetops, adverse wind shear will be directed downslope parallel to the failure plane. Downslope components of tree and soil loadings are used except when groundwater flow is assumed parallel to the failure plane; then pore water pressure does not enter shear force computation. Shear stress can then be represented as

$$\tau' = H \sin \beta \cos \beta \left[\frac{q_0}{H} + \frac{T_{\text{sw}}}{H \sin \beta \cos \beta} + \gamma_{\text{sat}} (M-Z^*) + \gamma(1-M) \right] \quad (10)$$

If τ = overall shear resistance and τ' = overall shear stress, the factor of safety equation can be written as

$$FS = \frac{R}{D} = \frac{\tau}{\tau'} \quad (11)$$

Substituting shear strength (Equation 9) and shear stress (Equation 10) into Equation 11 yields a factor of safety equation of

$$FS = \frac{Cs + Cr + H \cos^2 \beta \left\{ \left(\frac{q_0}{H} \right) + (\gamma_{sat} - \gamma_w) (M - Z^*) + \gamma (1 - M) \right\} \tan \phi}{H \left\{ \left(\frac{q_0}{H} \right) + (T_{sw} / H \sin \beta \cos \beta) + \gamma_{sat} (M - Z^*) + \gamma (1 - M) \right\} \sin \beta \cos \beta} \quad (12)$$

Parameters in Equation 12 can be placed into nondimensional groups as

$$FS = \frac{\frac{2(Cs + Cr)}{\gamma_w H \sin 2\beta} + \left[\frac{q_0}{\gamma_w H} + \left(\frac{\gamma_{sat}}{\gamma_w} - 1 \right) (M - Z^*) + \frac{\gamma}{\gamma_w} (1 - M) \right] \frac{\tan \phi}{\tan \beta}}{\frac{q_0}{\gamma_w H} + \frac{2T_{sw}}{\gamma_w H \sin 2\beta} + \left(\frac{\gamma_{sat}}{\gamma_w} \right) (M - Z^*) + \frac{\gamma}{\gamma_w} (1 - M)} \quad (13)$$

As Equation 13 shows, the basic model contains variables for four factors present in a forested area. Representing soil factors are γ , γ_{sat} , Cs , and ϕ ; all controlled by soil type, while H = a measure of soil depth. Topography is included as slope inclination, β . Vegetative factors are q_0 , Cr , and T_{sw} . Finally, a dynamic factor for relative groundwater level is included as M . This basic equation is used to derive a more simplified form.

Using sensitivity and order of magnitude analysis techniques, Ward (1976) showed the factor of safety (Equation 13) could be reduced to an accurate, simpler form by determining that certain variables were relatively unimportant and others could be assumed as constants. Relative depth, Z^* , was set at zero for the worst case. Wind shear, T_{sw} , was determined insignificant in magnitude, and soil mass and tree loading terms had little effect on the sensitivity of the equation. Soil and tree loading could have either positive or negative effects on slope stability depending on other factors. The simplified infinite slope factor of safety model used in this study for estimating landslide potential is then

$$FS = \frac{\frac{2(Cs + Cr)}{\gamma_w H \sin 2\beta} + \left[\frac{q_0}{\gamma_w H} + \left(\frac{\gamma_{sat}}{\gamma_w} - 1 \right) M + \frac{\gamma}{\gamma_w} (1 - M) \right] \frac{\tan \phi}{\tan \beta}}{\frac{q_0}{\gamma_w H} + \left(\frac{\gamma_{sat}}{\gamma_w} \right) M + \frac{\gamma}{\gamma_w} (1 - M)} \quad (14)$$

Equation 14 defines the landslide potential of a slope in terms of a factor of safety value. For relative rankings of hazards, limits of factor of safety values can be established considering possible errors in the variables. Relative errors in factor of safety values can be approximately 20 to 30 percent (Ward, 1976), comparable to results of others (Feld, 1965; Singh, 1971). A realistic set of relative hazard levels is given in Table 1, column 2. Although other limits could be selected, these values were considered most appropriate for the cases under examination.

Table 1. Model classification of landslide potential and probability.

Classification (1)	Landslide Potential FS (2)	Landslide Probability P[FS < 1] (3)
High	< 1.2	> 60%
Medium	1.2-1.7	30-60%
Low	> 1.7	< 30%

Derivation of Probability Delineation

Soil and root strength parameters are highly variable or uncertain. Other parameters such as soil depth, slope angle, unit weight of soil, and groundwater depth can be estimated and set at some conservative value. If groundwater level, M , is assumed at a steady state, and H , β , and γ are known, the factor of safety equation can be simplified to

$$FS = L_1(C_s) + L_1(C_r) + L_2(\tan\phi) \quad (15)$$

where

$$L_1 = \frac{2}{\gamma_w H \sin 2\beta \left[\left(\frac{q_0}{\gamma_w H} \right) + \left(\frac{\gamma_{sat}}{\gamma_w} \right) M + \left(\frac{\gamma}{\gamma_w} \right) (1-M) \right]} \quad (16)$$

and

$$L_2 = \frac{\left(\frac{q_0}{\gamma_w H} \right) + \left(\frac{\gamma_{sat}}{\gamma_w} - 1 \right) M + \left(\frac{\gamma}{\gamma_w} \right) (1-M)}{\left[\left(\frac{q_0}{\gamma_w H} \right) + \left(\frac{\gamma_{sat}}{\gamma_w} \right) M + \left(\frac{\gamma}{\gamma_w} \right) (1-M) \right] \tan \beta} \quad (17)$$

If Equation 14 is rewritten in terms of random variables, it becomes

$$S = L_1 X + L_1 Y + L_2 Z \quad (18)$$

where S , X , Y , and Z are the random variables. The expected value, $E[\cdot]$, or the mean of a linear equation such as Equation 18 is (Benjamin and Cornell, 1970)

$$E[S] = L_1 E[X] + L_1 E[Y] + L_2 E[Z] \quad (19)$$

If the strength parameters are considered independent (Holtz and Krizek, 1971; Lumb, 1970), the variance, $\text{Var}[\cdot]$, or standard deviation squared becomes

$$\text{Var}[S] = E[(S - E[S])^2] \quad (20)$$

or

$$\text{Var}[S] = E[S^2 - 2E[S]S + E^2[S]] \quad (21)$$

Following the form of Equation 19, Equation 21 becomes

$$\text{Var}[S] = E[S^2] - 2E[S] \cdot E[S] + E^2[S] \quad (22)$$

because

$$E[E[S]] = E[S].$$

Equation 22 reduces to

$$\text{Var}[S] = E[S^2] - E^2[S] \quad (23)$$

The term S^2 is defined as

$$S^2 = L_1^2 [X^2 + 2XY + Y^2] + L_1 L_2 2Z[X + Y] + L_2^2 Z^2 \quad (24)$$

Substitution of Equation 24 into Equation 23 yields

$$\begin{aligned} \text{VAR}[S] &= L_1^2 [E[X^2] + 2E[X]E[Y] + E[Y^2]] \\ &\quad + 2L_1 L_2 E[Z] [E[X] + E[Y]] + L_2^2 E[Z^2] - E^2[S] \end{aligned} \quad (25)$$

Following the form of Equation 22, the substitution for $E[X^2]$ can be made as

$$E[X^2] = \text{Var}[X] + E^2[X] \quad (26)$$

Similar substitutions are made for Y and Z yielding

$$\begin{aligned} \text{Var}[S] &= L_1^2 [\text{Var}[X] + E^2[X] + 2E[X]E[Y] + \text{Var}[Y] + E^2[Y]] \\ &\quad + 2L_1 L_2 E[Z] [[E[X] + E[Y]] + L_2^2 [\text{Var}[Z] + E^2[Z]] \\ &\quad - E^2[S] \end{aligned} \quad (27)$$

The mean and variance computed from Equations 9 and 26 can be used to estimate failure probability. This is written as

$$P[FS \leq 1] = p \quad (28)$$

where p = probability of failure and $P[FS \leq 1]$ = cumulative probability that FS is less than or equal to one. A reasonable distribution of failure probabilities is a normal or Gaussian distribution. Making this choice allows computation of the failure of probability. First, a nondimensional variate, U , is computed as

$$U = \frac{1 - \overline{FS}}{(\text{Var [FS]})^{1/2}} \quad (29)$$

The value of U is used to compute cumulative failure, p , as

$$p \cong 0.4 U \quad \text{if } U \leq 0.13 \quad (30)$$

or

$$p \cong -0.01314 + 0.49494 U - 0.15804 U^2 + 0.01661 U^3 \quad \text{if } U > 0.13 \quad (31)$$

Equations 29 and 30 are approximations with errors less than one percent.

From U and B the failure probability is found as

$$P[FS \leq 1] = 0.5 + p \quad \text{if } U > 0 \quad (32)$$

$$P[FS \leq 1] = 0.5 - p \quad \text{if } U < 0 \quad (33)$$

$$P[FS \leq 1] = 0.5 \quad \text{if } U = 0 \quad (34)$$

Similar to potential rankings, probabilities can be grouped into three hazard classes, as shown in Table 1, column 3. These limits can be modified depending upon the case under examination. Please note, however, that a high potential is not necessarily identical with high probability. The levels in Table 1 are not one-to-one correlations.

The means and variances of C_s , C_r , and $\tan \phi$ must be known or estimated to find failure probability. Usually this type of information is not available to the engineer without extensive measurements. Ward (1976) and Ward, Li, and Simons (1978) suggest that input variables be assumed as uniformly distributed random values. With this assumption, the mean of a random number is found as

$$E[X] = \frac{X_a + X_b}{2} \quad (35)$$

and the variance as

$$\text{Var [X]} = \frac{(X_b - X_a)^2}{12} \quad (36)$$

where X_a and X_b = lower and upper limits on the variable X .

Ward, Li, and Simons (1978) used Monte Carlo generation techniques to demonstrate that the assumption of a uniform distribution provided a more conservative estimate or overestimate of failure probability. Another appealing aspect of the uniform distribution assumption is that a range of values can be chosen as the input. Ward (1976) presented tentative sets of ranges for C_s , ϕ , and C_r based on the Uniform Soil Classification and vegetative characteristics. These values are guidelines and are subject to modification by the user.

Tree root cohesion represents the tensile and shear resistance of the roots and may vary significantly. Although some research indicates values up to 250 psf, Burroughs and Thomas (undated) suggest tree root strengths of 2856 psf for Douglas fir growing in Tye sandstone basins. However, tree roots are only effective if the failure surface intersects them. In deep seated slides, the failure surface is often below the roots. In instances of planar type landslides, the roots are effective only if they connect the soil mass to the underlying stable strata. Although considered as a beneficial influence to slope stability, tree roots only enhance stability under certain conditions.

Model Sensitivity

An important aspect of any mathematical model is its sensitivity to various input variables. Often it is desirable to know how accurately an input must be measured or the effect of changing the value of a variable on a model's output. Ward (1976) used partial differentiation of the factor of safety equation to demonstrate model response to changes in each input variable.

Under certain conditions, an increase in the value of an input variable can produce positive, negative, or no change in the FS value. These types of relationships occur for γ , γ_{sat} , q_0 , and H . The soil depth measure, H , usually has a negative influence on FS except for a dry cohesionless slope where $FS = \frac{\tan\phi}{\tan\beta}$. It can be demonstrated mathematically that increasing γ , γ_{sat} , and q_0 may beneficially effect slope stability under certain conditions. Mathematically, this would occur when

$$C_s + C_r < \gamma_w H_w \tan\phi \cos^2\beta \quad (37)$$

Theoretically, when conditions exist that satisfy this inequality, uniform loading of a slope should increase stability. This result suggests that in some cases forests aid stability by adding a uniform load to the soil. The relative importance of each variable can be graphically displayed through numerical computation of FS values using different variable values. For a selected set of conditions, some inputs have a linear effect on FS values while others, notably H and β , have strong nonlinear effects. Graphs are useful for showing the relative importance of each variable as compared to others (Figure 3). Although this figure is for a selected set of values, computations for other input sets show the same relative shapes. Sometimes C_s and C_r reverse their relative importance and q_0 , not shown, becomes slightly more important. In most cases, γ has only a slight affect as do γ_{sat} and q_0 . These three variables have smaller effects for reasons previously explained but also because they are included in the numerator (resisting force) and denominator (driving force) of Equation 14. This type of analysis is important in studying a new area since it indicates which input variables are most important to measure and what variable changes most affect stability.

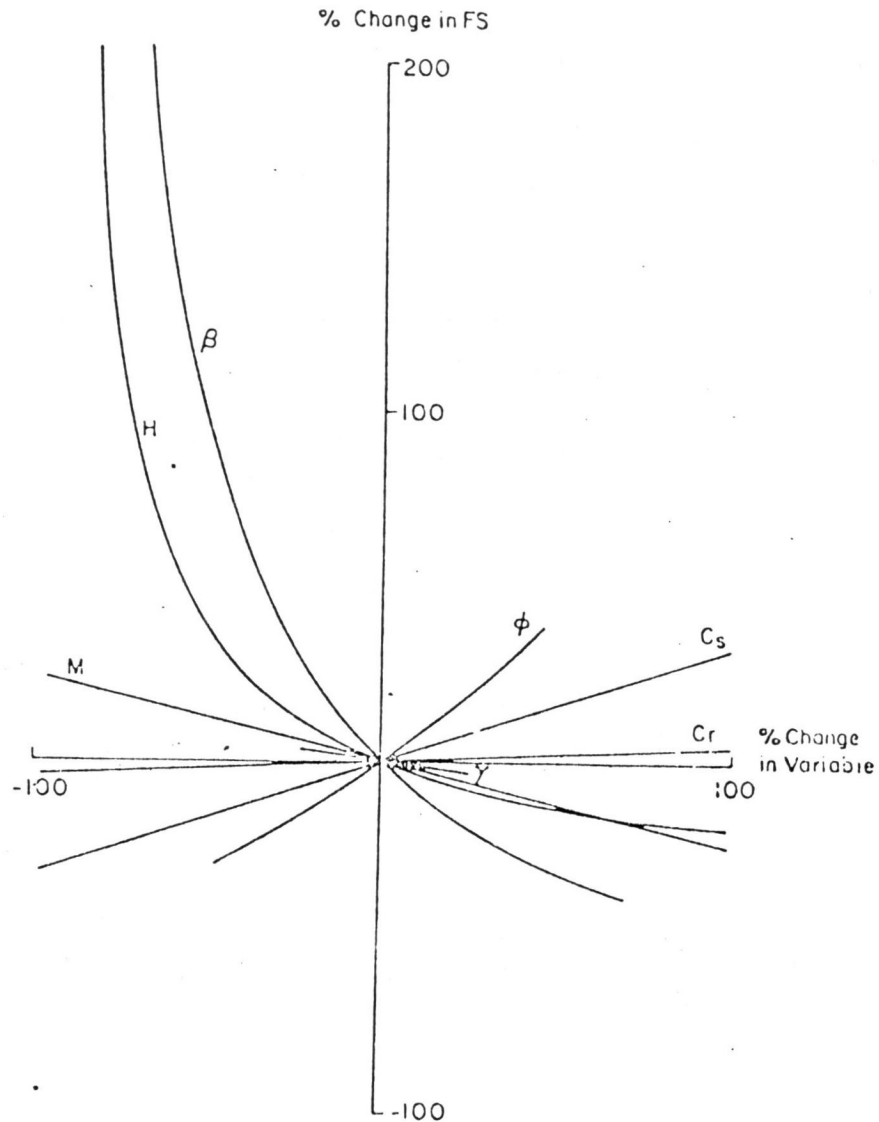


Figure 3. Percent change in factor of safety, FS, as compared to percent change in variable.

COMPUTER MAPPING OF WATERSHED LANDSLIDE HAZARDS

Background

The landslide potential and probability model together with a realistic range of input values allows analysis of slope stability. Such an approach is adequate for small areas but large areas require computer-based models to process extensive quantities of input data and simulate short- and long-term changes. Another desirable feature of computer-based system response models is the ability to process and utilize information from remote sensing sources.

In the landslide mapping model, watersheds are segmented and digitized for analysis using a watershed segmentation model developed by Simons and Li

(1975). With this model, a grid system subdivides the watershed into square or rectangle response units, also called cells. Cell size depends on the accuracy required for the output data, size of the area to be mapped, quality of input data, use of the output, and whether mapping will reflect land-use changes.

Data input is fairly general. A cell size is selected and the corresponding grid is overlaid on the raw data maps (Figure 4). Some maps are composed entirely of code numbers that designate various characteristics. For example, if the raw data shows vegetation, code number 1 may indicate high root strength while number 2 may indicate low root strength. Code data input at the grid line intersections or nodes allows assignation of values to the respective variables. This procedure is followed for vegetation and soil but other data such as elevation or canopy density (the relative amount of vegetation) are input as raw numbers and are not coded. With data input and stored, the segmentation model computes several useful quantities. Elevation data is used to compute slope inclination and aspect of the cell. Slope aspect indicates the direction the cell slopes; that is, the direction of landslide movement in the cell. The watershed segmentation program organizes data on a cell-by-cell basis for the watershed. The organized, coded, and averaged values are then output to a mass storage device or permanent file where they are accessed by the landslide hazard mapping program.

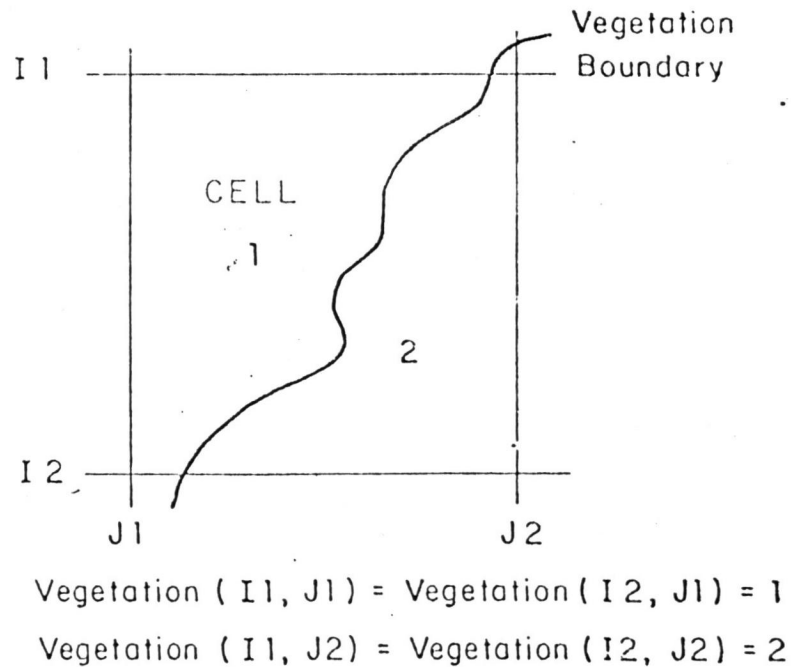


Figure 4. Input format to segmentation model.

Landslide Hazard Mapping

Output from the segmentation model (WASEG) is input to the landslide hazard mapping program (LSMAP). In the basic version, LSMAP requires input from program WASEG and the user. A more detailed version incorporates WASEG, LSMAP, and gray map printing routines into a method for delineating landslide hazards as well as other watershed characteristics.

Program LSMAP analyzes the watershed on a cell-by-cell basis. Soil and root strength values and soil depths are averaged for each cell. Consequently, the factor of safety is based on the averaged values for each cell, rather than the average of the factors of safety at each node point.

The landslide hazard mapping model presented here can provide a rapid means of assessing the impacts of various land-use changes on slope stability. An application using actual field data is presented in the following section.

APPLICATION OF MODEL

Site Selection

A heavily forested, landslide-prone watershed was selected for analysis. The selected watershed is located in the H. J. Andrews Experimental Forest about 50 miles east of Eugene, Oregon on the western edge of the Cascade Range and is shown in the topographic map supplied by Fred Swanson, USDA Forest Service, Oregon State University (Figure 5). Watershed 2 with an area of approximately 149 acres is located in the southwest corner of the Experimental Forest. Elevations in the area range from about 1730 to 3500 feet above mean sea level with slopes often in excess of 80 percent.

Vegetation of the watershed is typical of the area. The canopy is primarily Douglas-fir in the 125-year age class (second-growth), 450-year age class (old-growth), or a combination of the two classes (Hawk and Dyrness, undated). In some locations, however, Western Red cedar and Hemlock are present. The geology of the watershed has been characterized as lava flows, welded and unwelded tuffs and pyroclastic flows, and water-worked volcanic sediments (Swanson and James, 1975). Almost all of the landslide activity is confined to the altered volcanoclastic rocks with little activity occurring in the lava flows (Swanson and Dyrness, 1975). Soils in this area are weathered from the underlying volcanic rocks (Dyrness, 1969; Hawk and Dyrness, undated; Paeth, et al., 1971) and can be grouped into five broad classes. Five groups were used to account for subtle but important variations in soil depth and relative stability that produced unrealistic results when only three groupings were used.

The estimated Unified Soil Classifications for the soils were ML, CL, and CH. These assumed classifications were used for initial estimates of soil strength parameters as outlined by Ward (1976). Distribution of these soils indicates that two groups predominate in the watershed (Figure 6).

A vegetation grouping was conducted on Watershed 2. Because the canopy is well developed, it was assumed the root system was also well developed. Therefore, classification of vegetation with respect to characteristic root strength was based on a combination of the canopy cover densities of the larger overstory trees and the smaller understory trees and brush. Cover percentages provided a method of classification for root strength. Most of Watershed 2 was characterized by vegetation groups of second and old growth plant communities (Figure 7).

Runoff from the watershed is controlled by groundwater discharge. Precipitation averages nearly 90 inches per year with about 90 percent of the

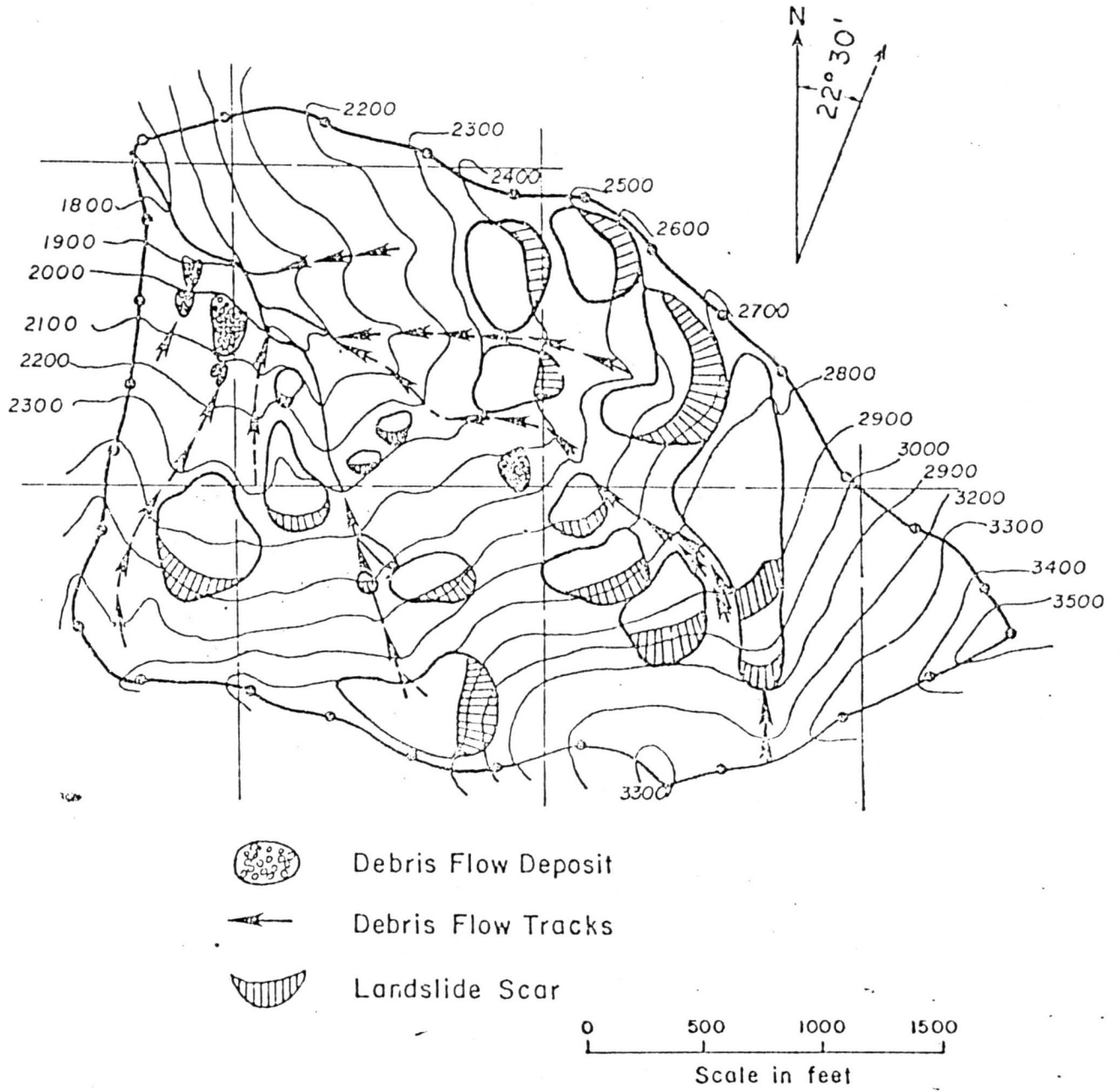


Figure 5. Topographic map of Watershed 2 showing landslide scars and deposits.

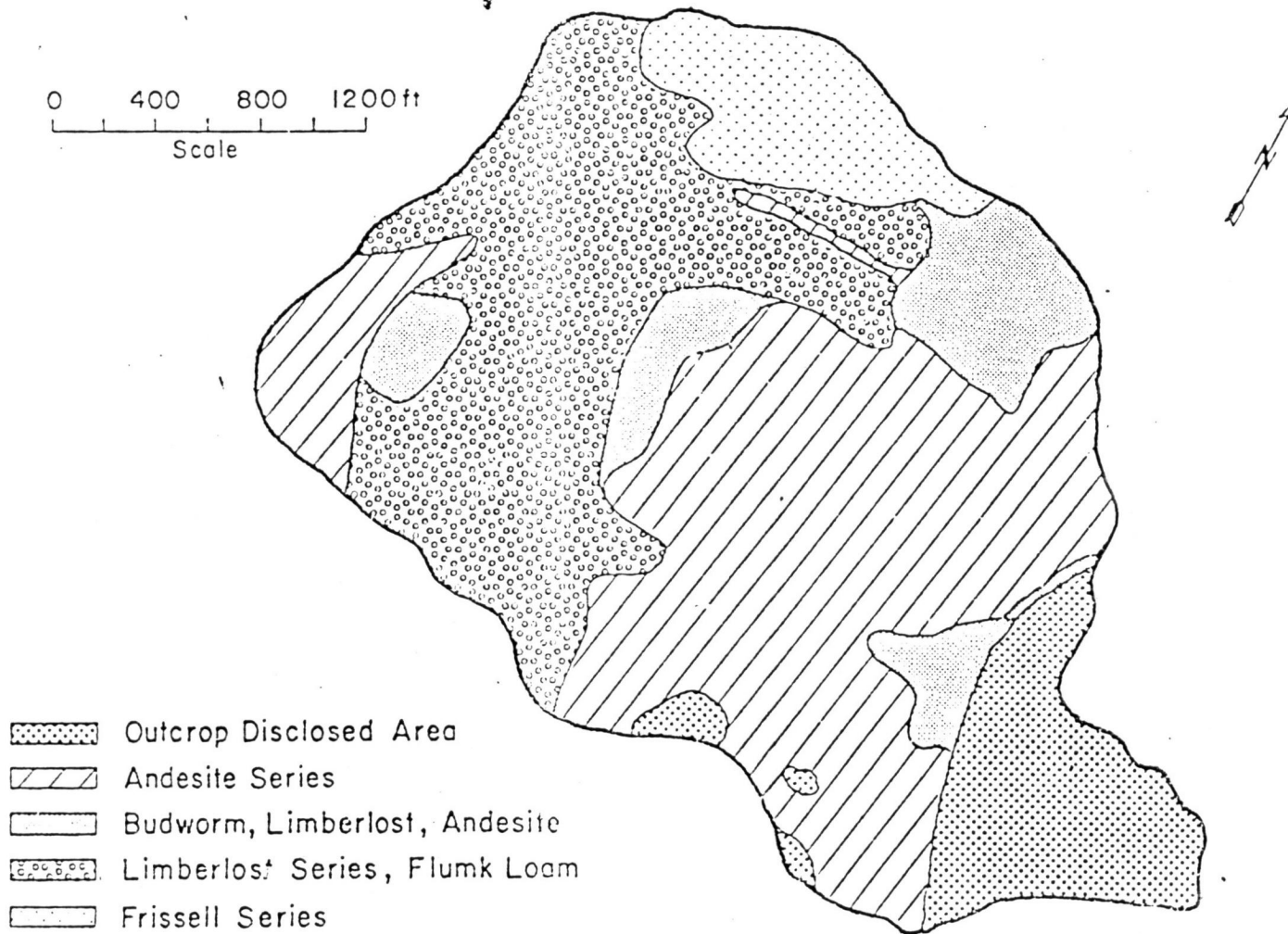
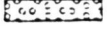
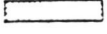


Figure 6. Soil classification map of Watershed 2 (after Hawk and Dyrness, undated).

-  Second and Old Growth Mix Cover $\geq 75\%$
-  Old Growth Cover 50-75%
-  Second Growth Community Cover
-  Old Growth Less than 25%
-  Vine Maple Open

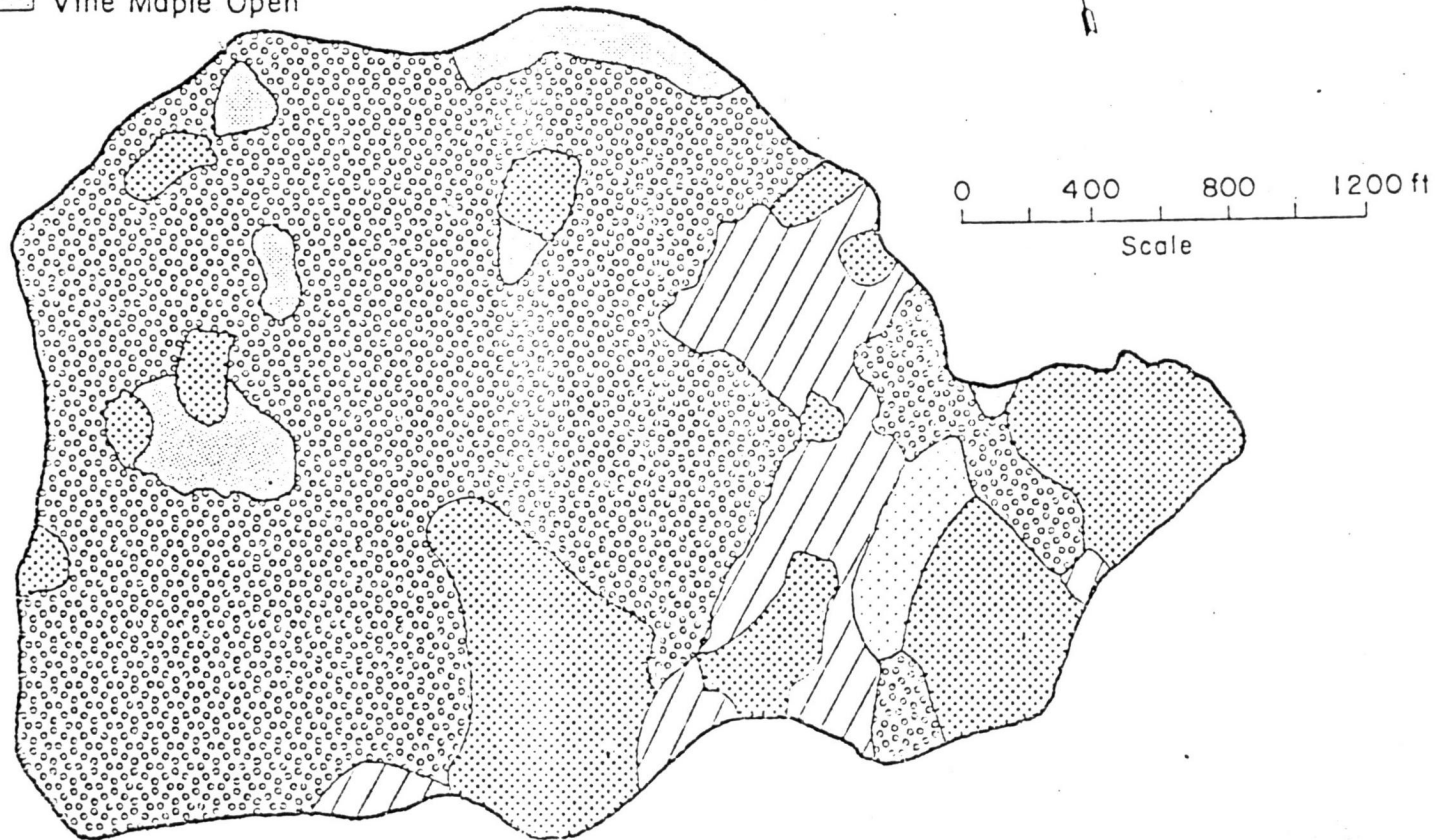


Figure 7. Vegetation map of Watershed 2 (after Hawk and Dyrness, undated).

total occurring as rainfall from October to April. Storms may last several days producing rainfall of several inches. Rainfall intensities are usually low and soil infiltration rates high, therefore, overland flow seldom occurs. Streamflow is fed primarily by saturated and unsaturated groundwater flow. Because of the importance of groundwater in slope stability, it was recognized that fluctuations in the groundwater table during a storm were important. Unfortunately, an acceptable, easily applied groundwater model was not available for use in this application, therefore, only selected levels were utilized for comparison.

The segmented watershed with the superimposed grid system is shown in Figure 8. Code values were input for the five soil classes and vegetation types along with elevations and cover densities. These codes start in the lower left corner and continue counterclockwise. For example, the vegetation code in Figure 4 is 1221.

In Watershed 2, 78.5 cells (0.5 cells for a cell near a stream channel) of 181 cells in the segmented watershed were denoted as having mappable landslide scars and deposits. These hazard cells were used as a guide to model performance and adjustment. If the model predicted a potential landslide hazard in these cells, it is accepted as a correct result. Overestimation or underestimation of the number of hazardous cells indicates: a) some hazardous cells may have negative characteristics and consequently are mapped as non-hazardous, b) cells mapped as hazardous but not containing landslides may be near failure, or c) the model is incorrect due to erroneous data. Comparison of the number of correct classifications with incorrect classifications for initial runs indicated the physical process model reflected the correct slope stability conditions.

The model was adjusted through soil and root strength parameters to better match the observed data. Two criteria were established to this adjustment. First, under typical soil moisture conditions no cell should fail. Second, under saturated conditions all the landslide cells should fail. Although failure may occur in all the landslide cells before saturation, data does not indicate at what level failure occurred. Using these two criteria, the input values were adjusted over realistic ranges. These values plus others used in the model are listed in Table 2.

Low values of cohesion and friction angle for soil classes 2 and 3 were consistent with field observations of failures in these soils. Higher values for the other three soil classes reflect the relative stability associated with those groupings. Similar considerations were used when selecting proper ranges of root strengths. No formal methodology was used for arriving at the adjusted values in Table 2. The values do, however, reflect the relative stability of groups they represent.

The adjusted model indicated a total of 81.5 hazardous cells, 69 of which corresponded with the assumed hazardous cells, an 87.9 percent match. A total of 9.5 cells were classed as safer than assumed and 12.5 were classed as more hazardous. This is encouraging since it indicates the model represents the physical processes controlling landslide occurrence.

The adjusted model was then used to study dynamic changes in the watershed. The first application showed the change in landslide hazards under

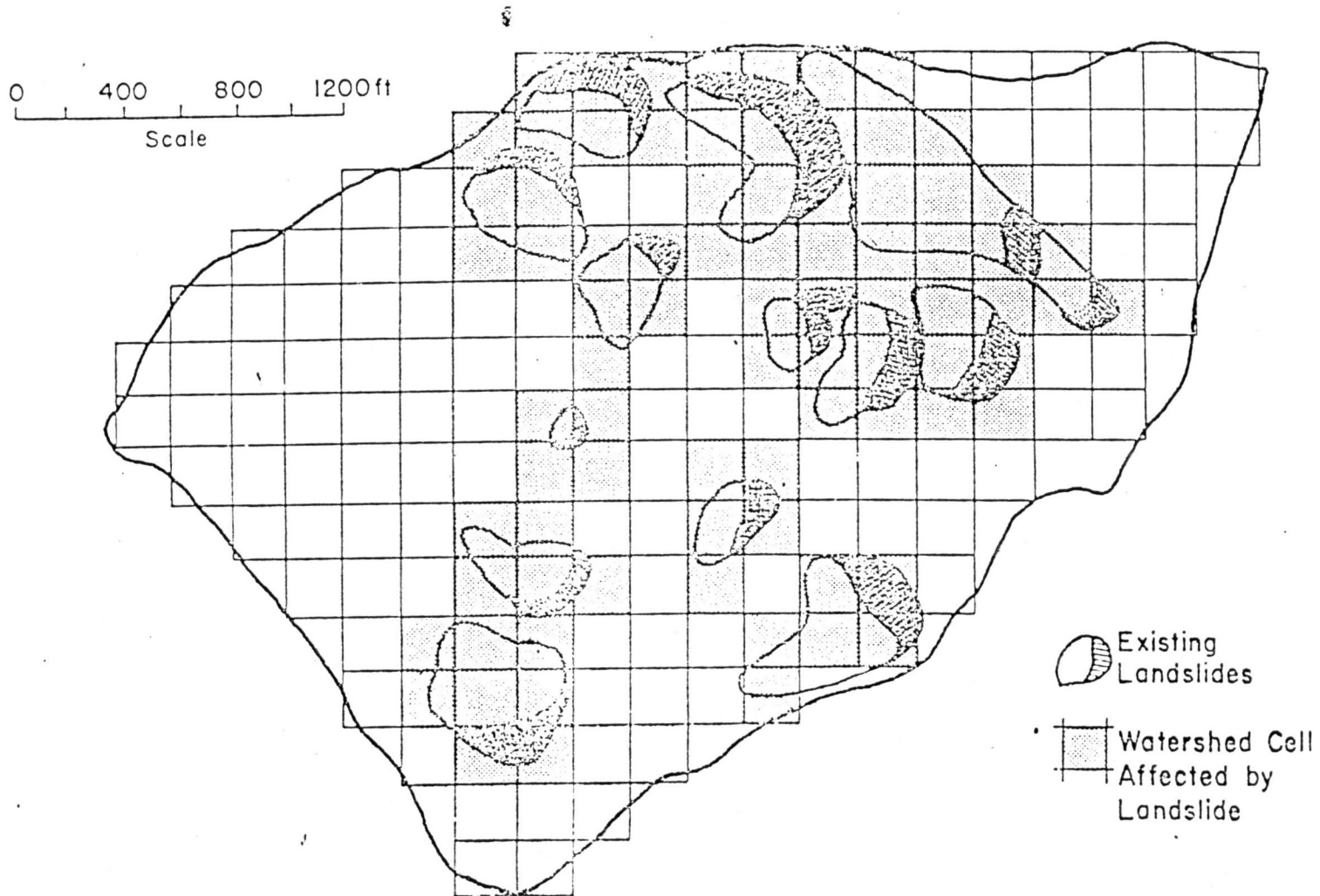


Figure 8. Watershed Number 2: existing landslides and watershed cell system.

Table 2. Input values for LSMAP.

Soil porosity = 0.60 Dry unit weight of soil = 66.1 pounds per cubic foot Saturated unit weight of soil = 103.6 pounds per cubic foot Vegetative surcharge = 50 pounds per square foot				
Soil Group (1)	Soil Names (2)	Cohesion Range, in pounds per square foot (3)	Friction Angle Range, in degrees (4)	Typical Depth in feet (5)
1	Rock outcrop	1000-2000	35-40	5
2	Andesite series	20-50	5-20	8
3	Budworm, Limberlost, Andesite (slope < 20%)	0-5	2-5	10
4	Limberlost, Flunky	150-200	25-28	5
5	Frissell	350-400	30-33	4
Vegetation Group (1)		Root Strength Range, in pounds per square foot (2)		
1		290-360		
2		220-260		
3		5-25		
4		100-125		
5		15-65		

varying groundwater conditions. The potentially hazardous landslide areas and their estimated failure probabilities for a relative groundwater level of 0.5 are shown in Figures 9 and 10. Even under these conditions there are numerous areas of high potential because of the overwhelming driving forces brought about by the steep terrain. As expected, rising groundwater levels increase landslide hazards (Figures 11 and 12). If a real-time groundwater level model were available, daily or seasonal fluctuations in landslide hazards could be determined. Use of the model in determining relative hazards with respect to groundwater levels is important in planning watershed activities. Based on model results, scheduling of activities may be better determined to coincide with lower landslide hazards. Roadways may also be better planned to avoid hazardous areas or indicate where stability enhancement is required.

Timbering is another dynamic watershed activity that can be assessed with the model. Landslide potential for a 50 percent clearing of the canopy cover is shown in Figure 13. Comparison of Figure 13 with Figure 9 shows adverse effects on slope stability produced by vegetation removal. Similarly, if the watershed is clear-cut, even more instability is produced (Figure 14). However, an instantaneous drop in root strength is assumed, which is incorrect. A more realistic approximation would be loss of strength with time. The model provides a method for assessing impact of this type of timbering activity on the watershed.

An important aspect of the model is estimating landslide probability. Use of both the potential and probability maps provides the land use manager with another means for analyzing impacts of watershed activities. In addition, the probability map aids interpretation of the potential map.

SUMMARY AND CONCLUSIONS

This paper has presented the need for delineating the hazardous landslide areas. Delineation techniques were discussed and a mathematical modeling approach was detailed. Application of the approach indicates its usefulness for determining landslide hazards in a watershed under varying natural and man caused conditions.

H. J. ANDREWS EXPERIMENTAL FOREST, OREGON

WATERSHED 2

RELATIVE GROUNDWATER DEPTH .500

MAP SCALE 1 TO 4500

SYMBOL SET USED FOR THIS GRAY MAP INDICATES:

- SAFETY FACTOR LESS THAN OR EQUAL TO 1.2 W
- SAFETY FACTOR GREATER THAN 1.2 AND LESS THAN 1.7 I
- SAFETY FACTOR GREATER THAN 1.7 .

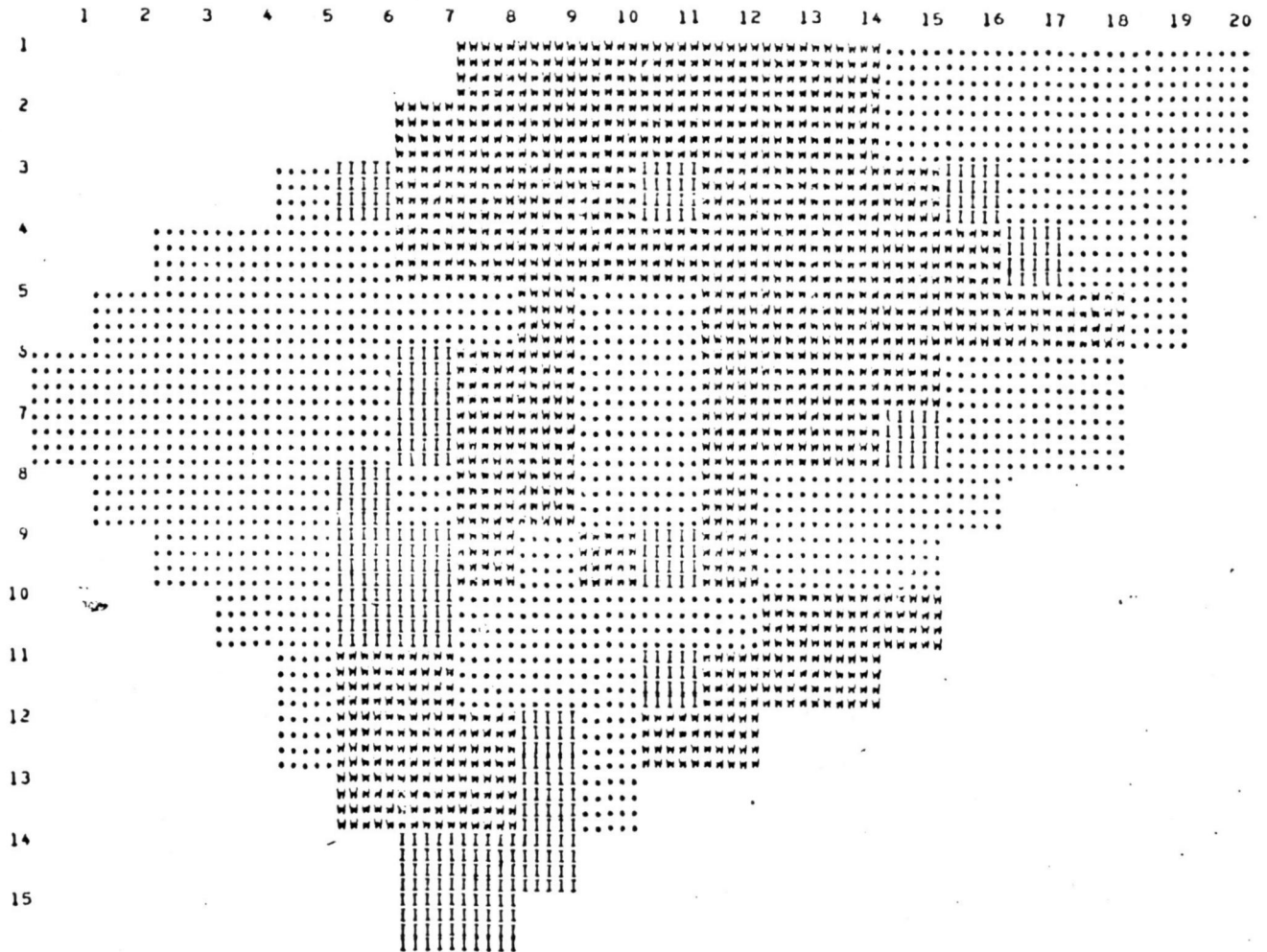


Figure 9. Gray map of potentially hazardous landslide areas for Watershed 2 with relative groundwater level of 0.5.

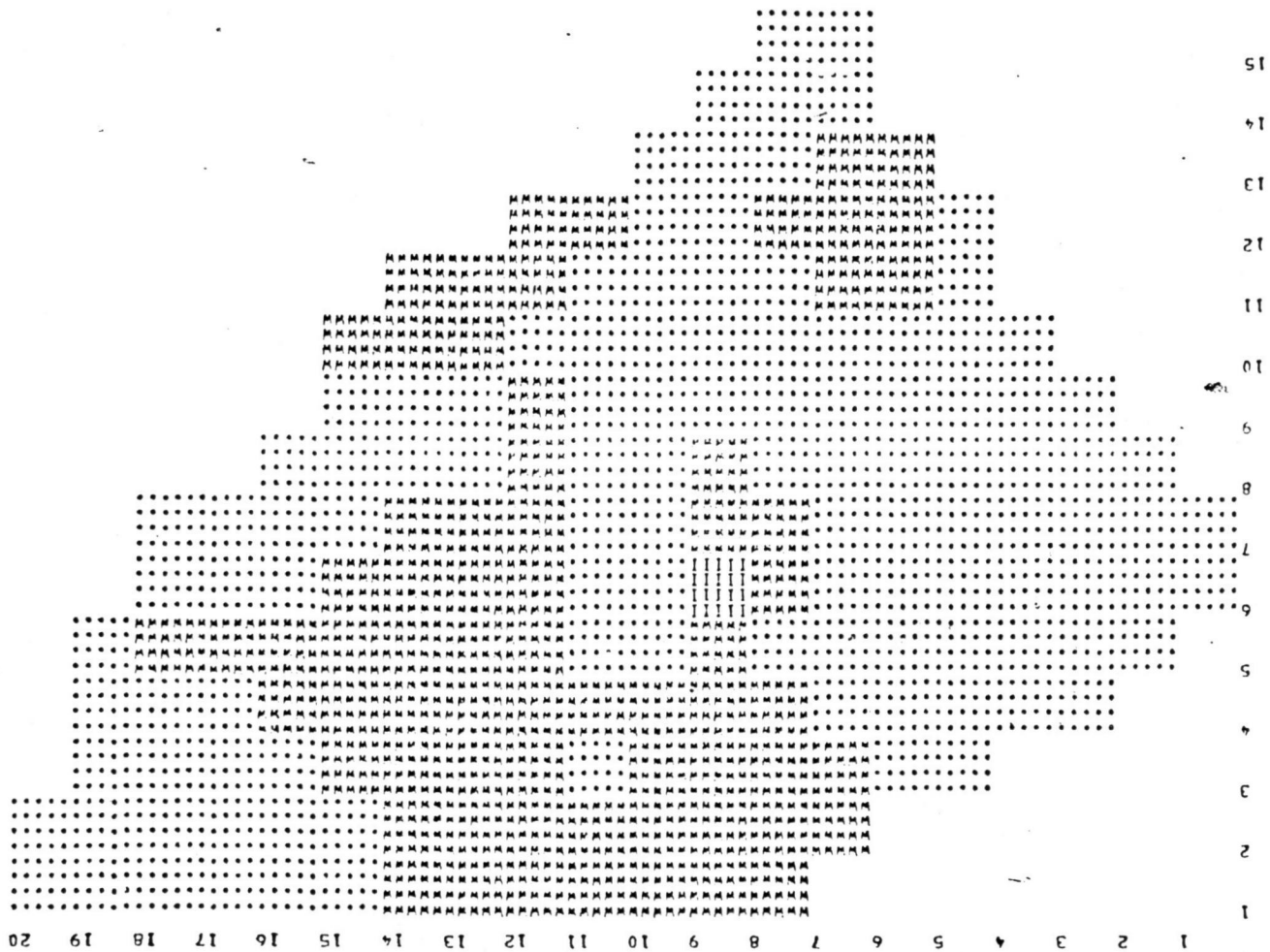


Figure 10. Gray map of estimated failure probabilities of landslide areas for Watershed 2 with relative groundwater level of 0.5.

M. J. ANDREWS EXPERIMENTAL FOREST, OREGON
 WATERSHED 2
 RELATIVE GROUNDWATER DEPTH .500
 MAP SCALE 1 TO 4800
 SYMBOL SET USED FOR THIS GRAY MAP INDICATES!
 M PROBABILITY OF SLIDING HIGHER THAN 60 PERCENT
 I PROBABILITY HIGHER THAN 30 PERCENT AND LESS OR EQUAL TO 60 PERCENT
 . PROBABILITY OF SLIDING LESS THAN 30 PERCENT

H. J. ANDREWS EXPERIMENTAL FOREST, OREGON

WATERSHED 2

RELATIVE GROUNDWATER DEPTH 1.000

MAP SCALE 1 TO 4800

SYMBOL SET USED FOR THIS GRAY MAP INDICATES:

SAFETY FACTOR LESS THAN OR EQUAL TO 1.2 W

SAFETY FACTOR GREATER THAN 1.2 AND LESS THAN 1.7 I

SAFETY FACTOR GREATER THAN 1.7 .

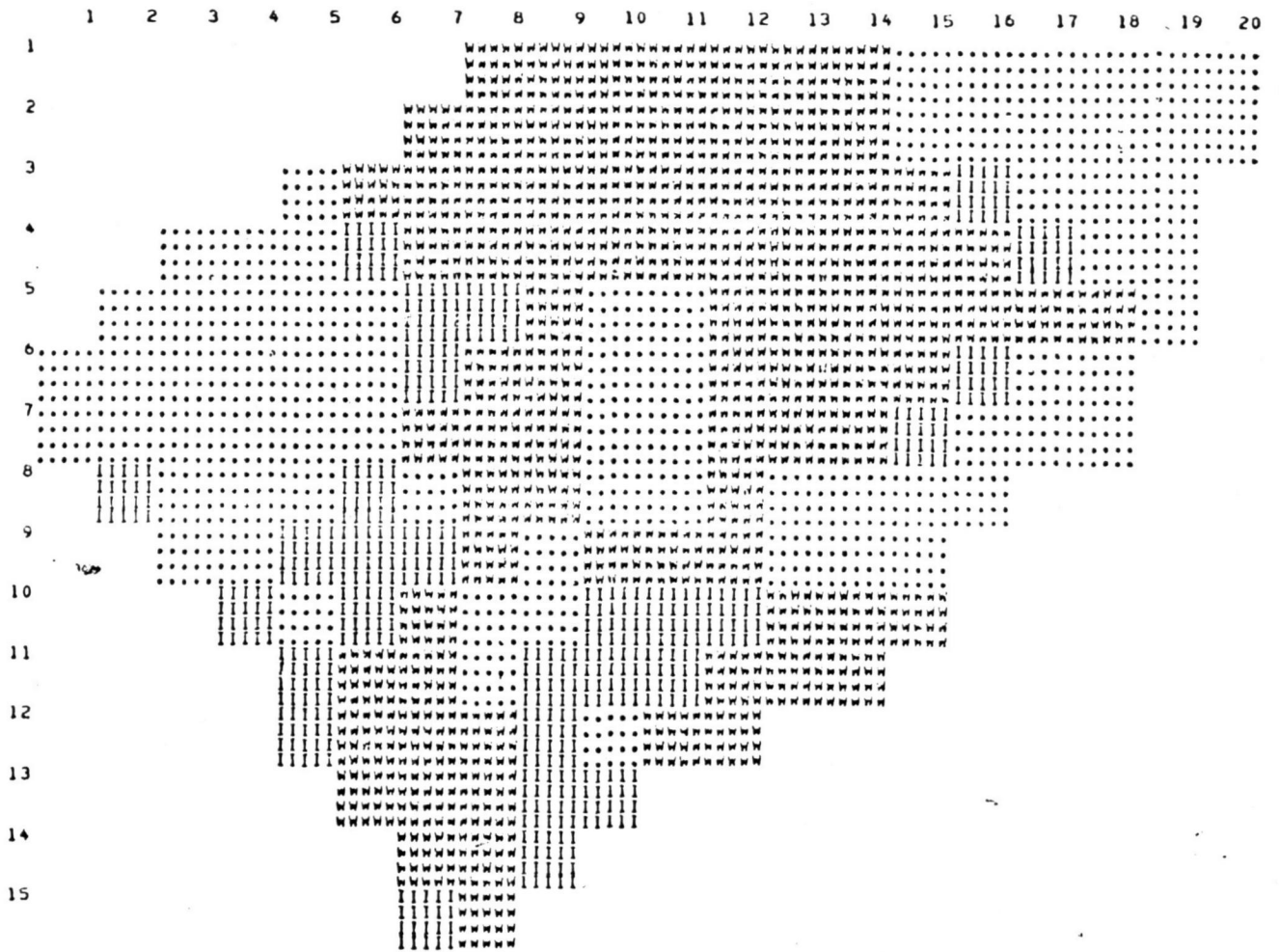


Figure 11. Gray map of potentially hazardous landslide areas for Watershed 2 with relative groundwater level of 1.0.

H. J. ANDREWS EXPERIMENTAL FOREST, OREGON

WATERSHED 2

RELATIVE GROUNDWATER DEPTH 1.000

MAP SCALE 1 TO 4800

SYMBOL SET USED FOR THIS GRAY MAP INDICATES:

- PROBABILITY OF SLIDING HIGHER THAN 60 PERCENT W
- PROBABILITY HIGHER THAN 30 PERCENT AND LESS OR EQUAL TO 60 PERCENT I
- PROBABILITY OF SLIDING LESS THAN 30 PERCENT .

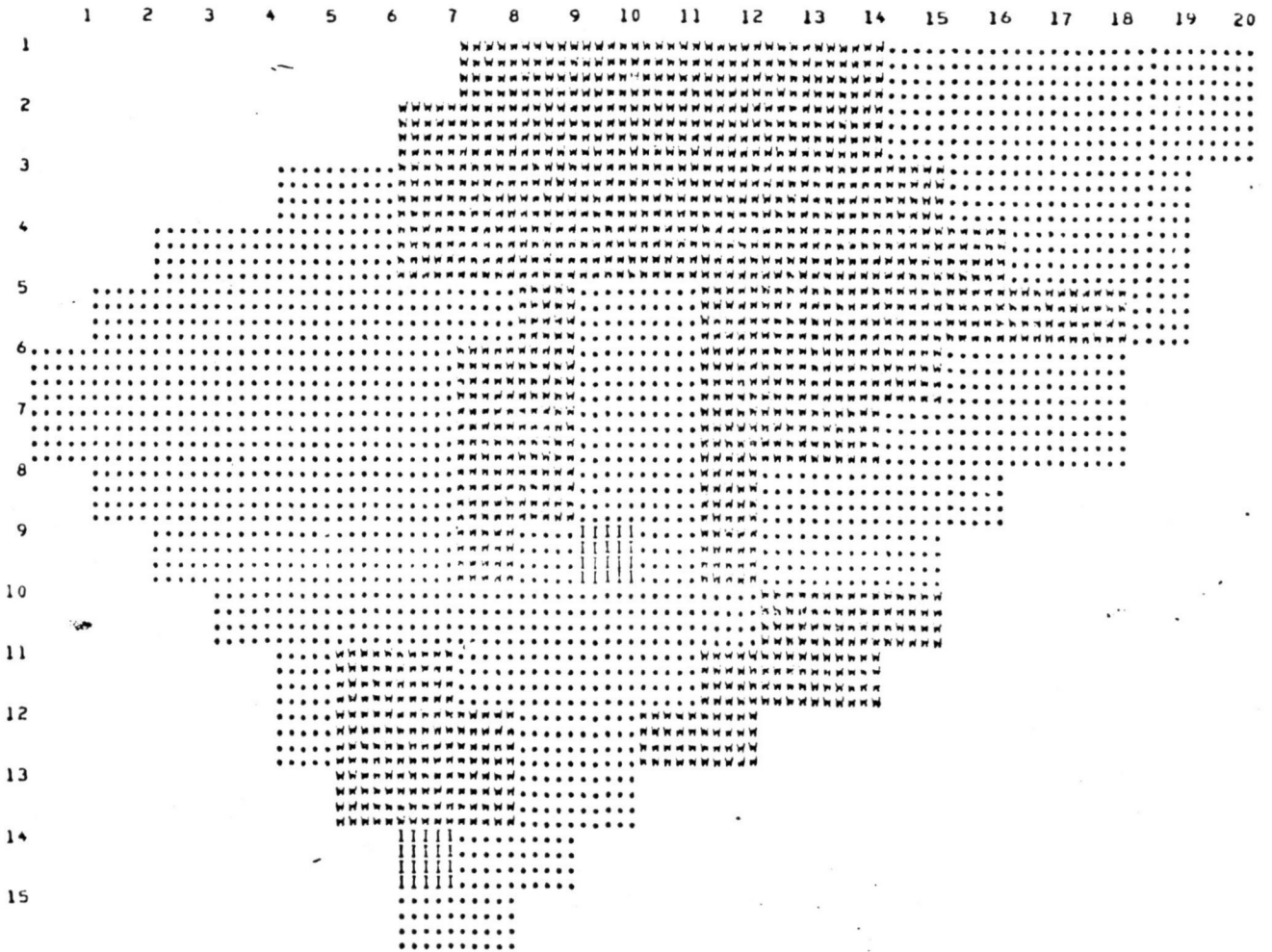


Figure 12. Gray map of estimated failure probabilities of landslide areas for Watershed 2 with relative groundwater level of 1.0.

M. J. ANDREWS EXPERIMENTAL FOREST, OREGON

WATERSHED 2

RELATIVE GROUNDWATER DEPTH .500

MAP SCALE 1 TO 4800

SYMBOL SET USED FOR THIS GRAY MAP INDICATES:

- SAFETY FACTOR LESS THAN OR EQUAL TO 1.2 W
- SAFETY FACTOR GREATER THAN 1.2 AND LESS THAN 1.7 I
- SAFETY FACTOR GREATER THAN 1.7 .

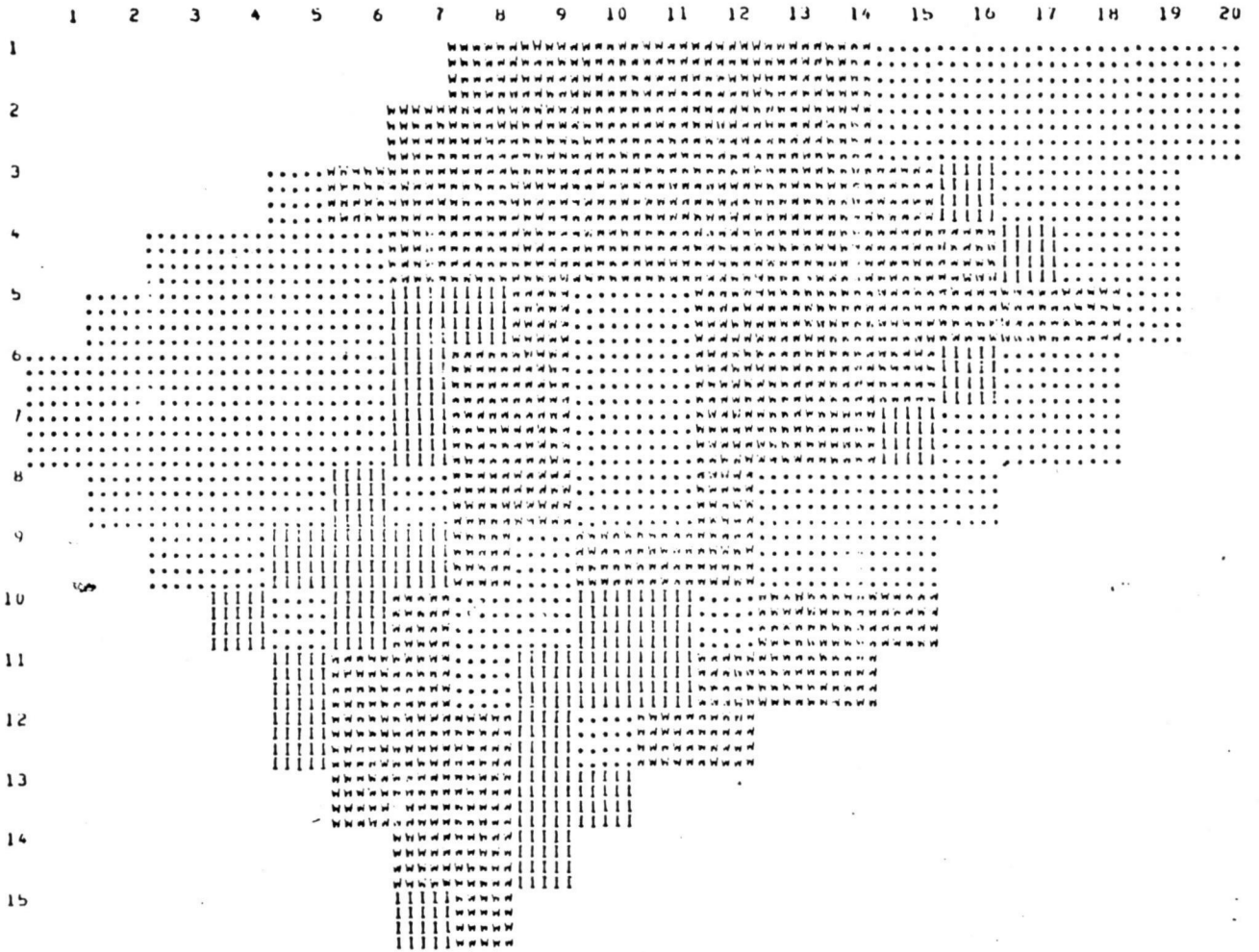


Figure 13. Gray map of potentially hazardous landslide areas for a 50 percent clearing of canopy cover with relative groundwater level of 0.5.

M. J. ANDREWS EXPERIMENTAL FOREST, OREGON

WATERSHED 2

RELATIVE GROUNDWATER DEPTH 0.500

MAP SCALE 1 TO 4800

SYMBOL SET USED FOR THIS GRAY MAP INDICATES:

- SAFETY FACTOR LESS THAN OR EQUAL TO 1.2
- ⊠ SAFETY FACTOR GREATER THAN 1.2 AND LESS THAN 1.7
- ◻ SAFETY FACTOR GREATER THAN 1.7

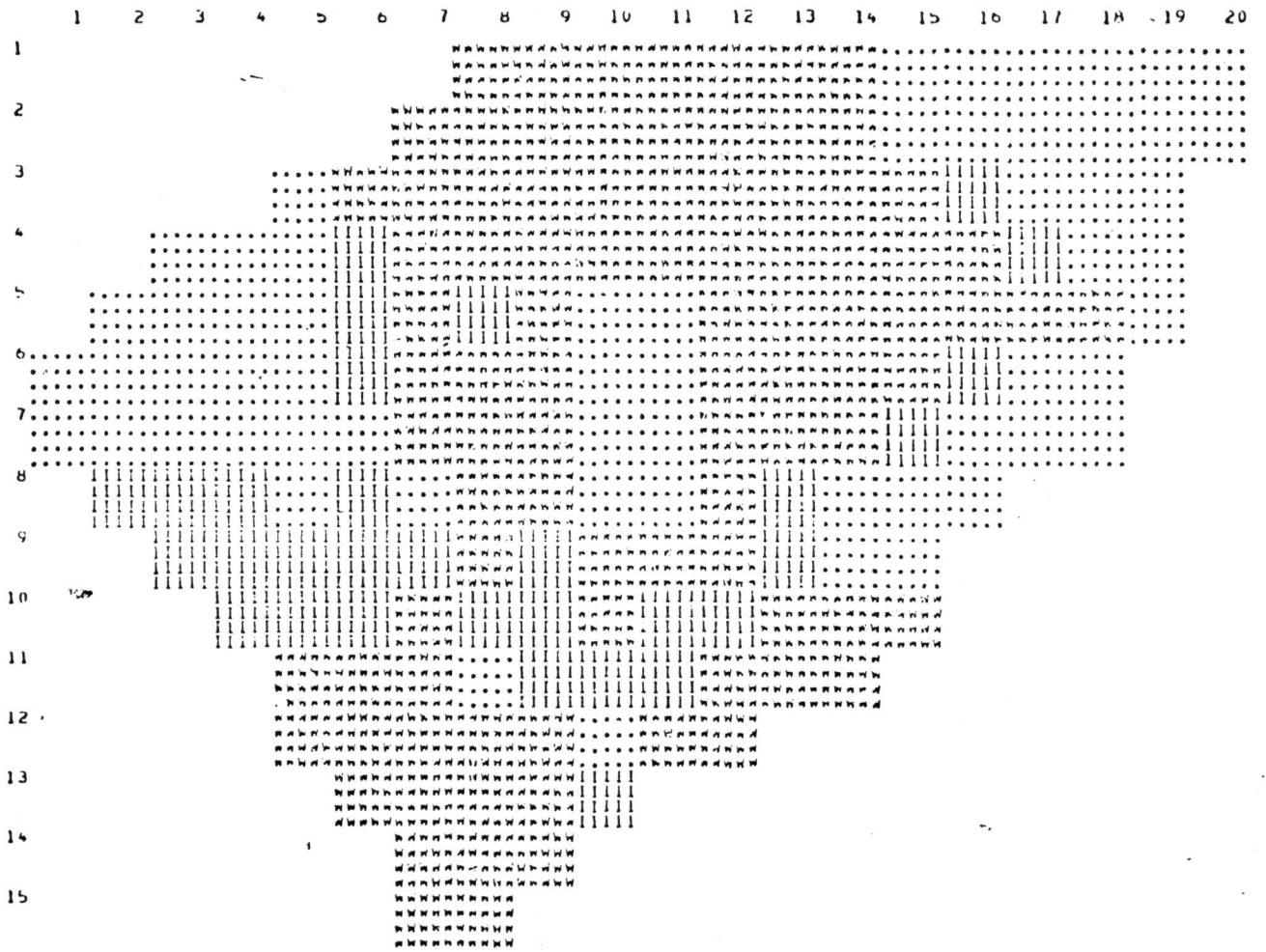


Figure 14. Gray map of potentially hazardous landslide areas for clear cut watershed with relative groundwater level of 0.5.

ACKNOWLEDGMENTS

The authors wish to thank the U.S. Department of Agriculture, Rocky Mountain Forest and Range Experiment Station, Flagstaff, Arizona and the Colorado State University Experiment Station for sponsoring projects from which this paper was derived.

REFERENCES

1. Baker, R. F., and Chieruzzi, R., "Regional Concept of Landslide Occurrence," Bulletin No. 216, Highway Research Board, 1959, pp. 1-16.
2. Benjamin, J. R., and Cornell, C. A., Probability, Statistics, and Decision for Civil Engineers, McGraw-Hill, New York, N.Y., 1970, pp. 147-150.
3. Blanc, R. P., and Cleveland, G. B., "Natural Slope Stability as Related to Geology, San Clemente Area, Orange, and San Diego Counties, California," Special Report 98, California Division of Mines and Geology, 1968.
4. Brown, C. and Sheu, M. S., "Effects of Deforestation on Slopes," Journal of the Geotechnical Engineering Division, ASCE, Vol. 101, No. GT2, Feb., 1975, pp. 147-165.
5. Building Research Advisory Board, National Research Council, National Academy of Sciences, "Methodology for Delineating Mudslide Hazard Areas," 1974.
6. Burroughs, E. R., and Thomas, B. R., "Initial Report for the Identification of Landslide Hazard Areas in Fyee Sandstone with Slope Gradients Exceeding Sixty Percent," Draft Report, U.S. Forest Service, unpublished, undated.
7. Chang, T. P., "Landslide Investigation Techniques," Colorado State University, Science Series No. 1, Department of Watershed Sciences, 1971.
8. Cleveland, G. B., "Regional Landslide Prediction," Open File Release 72-73, California Division of Mines and Geology, Sacramento, California, 1971.
9. Dyrness, C. T., "Hydrologic Properties of Soil on Three Small Watersheds in the Western Cascades of Oregon," Research Note PNW-111, U.S. Forest Service, Sept., 1969.
10. Endo, T., and Tsuruta, T., "On the Effect of Tree Roots Upon the Shearing Strength of Soil," Annual Report of the Hokkaido Branch Forest Experiment Station (In Japanese, English Summary), 1968.
11. Evans, J. R. and Gray, C. H., Jr., Eds., "Analysis of Mudslide Risk in Southern Ventura County, California," Open File Release 72-73, California Division of Mines and Geology, 1971.
12. Feld, J., "The Factor of Safety in Soil and Rock Mechanics," Proceedings, Sixth International Conference on Soil Mechanics and Foundation Engineering, Vol. 111, 1965, pp. 185-197.
13. Gray, D. H., "Effects of Forest Clearcutting on the Stability of Natural Slopes," Association of Engineering Geologists Bulletin, Vol. 7, Nos. 1 and 2, 1970, pp. 45-65.

14. Gray, D. H., "The Role of Woody Vegetation in Reinforcing Soils and Stabilizing Slopes," Proceedings, Symposium on Soil Reinforcing and Stabilizing Techniques in Engineering Practice, Sydney, Australia, October 13-16, 1978.
15. Hawk, G., and Dyrness, C. T., "Vegetation and Soils of Watershed 2 and 3," Internal Report 49, U.S. Department of Agriculture Forest Service, H. J. Andrews Experimental Forest, review copy, undated.
16. Holtz, R. D., and Krizek, R. J., "Statistical Evaluation of Soils Test Data," Proceedings, the First International Conference on Applications of Statistics and Probability to Soil and Structural Engineering, 1971, pp. 230-266.
17. Jones, F. O., Embody, D. R., and Peterson, W. L., "Landslides along the Columbia River Valley, Northeastern Washington," Survey Professional Paper 367, 1961.
18. Kryniene, D. P., and Judd, W. R., Principles of Engineering Geology and Geotechnics, McGraw-Hill, New York, N.Y., 1957, pp. 639.
19. Lambe, T. W., and Whitman, R. V., Soil Mechanics, John Wiley and Sons, New York, N.Y., 1969, pp. 352-373.
20. Liang, F. and Belcher, J. D., "Air Photo Interpretation in Landslides and Engineering Practice," Highway Research Board, Special Report No. 29, Publication 544, 1958.
21. Lumb, P., "Safety Factors and the Probability Distribution of Soil Strength," Canadian Geotechnical Journal, Vol. 17, No. 3, 1970, pp. 225-242.
22. McKean, J., "Density Slicing of Aerial Photography Applied to Slope Stability Studies," M.S. Thesis, Department of Earth Resources, Colorado State University, Fort Collins, Colorado, 1977.
23. Nilsen, T. H., and Brabb, E. E., "Current Slope-Stability Studies in the San Francisco Bay Region," Journal of Research, U.S. Geological Survey, Vol. 1, No. 4, July-Aug., 1973, pp. 431-437.
24. O'Loughlin, C., "The Effect of Timber Removal on the Stability of Forest Soils," Journal of Hydrology, Vol. 13, No. 2, New Zealand, 1974, pp. 121-134.
25. Paeth, R. C., et al., "Factors Affecting Mass Movement of Four Soils in the Western Cascades of Oregon," Proceedings, Soil Science Society of America, Vol. 35, No. 6, 1971, pp. 943-947.
26. Poole, D. H., "Slope Failure Forms: Their Identification, Characteristics and Distribution as Depicted by Selected Remote Sensor Returns," Proceedings, Sixth International Symposium on Remote Sensing of the Environment, Ann Arbor, Michigan, 1969.

27. Poole, D. H., "An Evaluation of the Utility of Remote Sensor Returns for a Study of Slope Failure Phenomena," Remote Sensing Institute Technical Report 14, East Tennessee State University, Johnson City, Tennessee, 1972.
28. Simons, D. B. and Li, R. M., "Watershed Segmentation by a Digital Computer for Mathematical Modeling of a Watershed," Draft Report, Rocky Mountain Forest and Range Experiment Station, Flagstaff, Arizona, Dec., 1975.
29. Simons, D. B. and Ward, T. J., "Landslide Potential Delineation," Civil Engineering Department, Engineering Research Center, Colorado State University, Fort Collins, Colo., Feb., 1976.
30. Simons, D. B., Ward, T. J., and Li, R. M., "Computer Application in Mapping Potential Landslide Sites," Proceedings, Summer Computer Simulation Conference, held at Washington, D.C., 1976.
31. Singh, A., "How Reliable is the Safety Factor in Foundation Engineering?" Proceedings, First International Conference on Applications of Statistics and Probability to Soil and Structural Engineering, Hong Kong University Press, 1971, pp. 390-424.
32. Swanson, F. J. and Dyrness, C. T., "Impact of Clear-cutting and Road Construction of Soil Erosion by Landslides in the Western Cascade Range, Oregon," Geology, Vol. 3, No. 7, 1975, pp. 393-396.
33. Swanson, F. J. and James, M. E., "Geology and Geomorphology of the H. J. Andrews Experimental Forest, Western Cascades, Oregon," Research Paper PNW-188, U.S. Department of Agriculture Forest Service, 1975.
34. Swanson, F. J., et al., "A Conceptual Model of Soil Mass Movement, Surface Soil Erosion, and Stream Channel Erosion Processes," Internal Report 72, Erosion Modeling Group, 1973.
35. Takada, Y., "A Geophysical Study of Landslides," Bulletin Disaster Prevention Research Institute, Kyoto University, Vol. 18, Part 2, No. 137, 1968.
36. Takeuchi, A., "Fractured Zone Type Landslide and Electrical Resistivity Survey - 1," Bulletin Disaster Prevention Research Institute, Kyoto University, Vol. 21, Part 1, No. 185, 1971.
37. Waltz, J. P., "An Analysis of Selected Landslides in Alameda and Contra Costa Counties, California," Association of Engineering Geologists Bulletin, Vol. 3, No. 2, 1971.
38. Ward, T. J., "Factor of Safety Approach to Landslide Potential Delineation," thesis presented to Colorado State University, at Fort Collins, Colorado, in August, 1976, in partial fulfillment of the requirements for the degree of Doctor of Philosophy.

39. Ward, T. J., Li, R. M., and Simons, D. B., "Landslide Potential and Probability Considering Randomness of Controlling Factors," Proceedings International Symposium on Risk and Reliability in Water Resources, University of Waterloo, Waterloo, Canada, June 26-28, 1978, pp. 592-608.

LIST OF SYMBOLS

C_r = root cohesion;
 C_s = soil cohesion;
 c = cohesion term;
 \bar{c} = effective cohesion;
 D = driving forces;
 $E[\]$ = expected value or mean of linear equation;
 FS = factor of safety;
 H = measure of soil depth;
 H^u = unsaturated soil height;
 H^w = saturated soil height or height to ground water table;
 L_1 = dimensionless grouping of parameters;
 L_2 = dimensionless grouping of parameters;
 M = relative groundwater height;
 n = number of soil layers;
 p = cumulative probability;
 P = probability of failure;
 q_0 = vegetative surcharge;
 R = resistive forces;
 S = random variable;
 T_{sw} = wind shear in trees;
 U = nondimensional variate;
 u = pore water pressure;
 $Var[\]$ = variance;
 \bar{x} = variable;
 \bar{x} = mean of variable x ;
 Y = random variable;
 Z = height above bedrock surface or random variable;
 Z^* = relative position above bedrock surface;
 β = slope inclination;
 γ = unit weight;
 Δz = thickness;
 Σ = summation sign;
 σ = total normal stress;
 $\bar{\sigma}$ = effective normal stress;
 τ = overall shear resistance;
 τ' = overall shear stress;
 ϕ = angle of internal friction;
 $\bar{\phi}$ = effective angle of internal friction.

Subscripts

a = area; lower limit;
 b = upper limit;
 i = layer i ;
 sat = saturated;
 w = water.